

We are IntechOpen, the world's leading publisher of Open Access books Built by scientists, for scientists

4,800

Open access books available

122,000

International authors and editors

135M

Downloads

Our authors are among the

154

Countries delivered to

TOP 1%

most cited scientists

12.2%

Contributors from top 500 universities



WEB OF SCIENCE™

Selection of our books indexed in the Book Citation Index
in Web of Science™ Core Collection (BKCI)

Interested in publishing with us?
Contact book.department@intechopen.com

Numbers displayed above are based on latest data collected.
For more information visit www.intechopen.com



Tropical Cyclone Wind-Wave, Storm Surge and Current in Meteorological Prediction

Worachat Wannawong¹ and Chaiwat Ekkawatpanit²

¹Earth System Science (ESS) Cluster,
The Joint Graduate School of Energy and Environment (JGSEE),
King Mongkut's University of Technology Thonburi, Bangkok,
²Department of Civil Engineering, Faculty of Engineering,
King Mongkut's University of Technology Thonburi, Bangkok,
Thailand

1. Introduction

Several researches in the earth system prediction have studied a delicate balance among ocean, land, ice, and atmosphere. The researchers have classified the scales in the meteorological prediction; the global, regional, coastal, synoptic, meso and other scales (Wittmann & Farrar, 1997). These discoveries raise new questions that now define the course of research for the coming three decades. From this scientific foundation, Earth System Science (ESS) cluster, The Joint Graduate School of Energy and Environment (JGSEE) must carefully formulate plans for requisite missions. The resultant next phase of research will extend our understanding of how ocean ecosystems, coastal sediment and erosion, coastal habitats, and hazards influence Earth's ecosystem health and services, human health, welfare, recreation, and commerce. ESS's Research Program will also enable the formulation of effective strategies for assessing, adapting to, and managing climate change through observations and improved Earth System modeling capabilities.

In this chapter, the recent events have illustrated the devastation and loss of human life, property, and commerce from environmental hazards that have impacted coastal zones (Fig. 1).



Fig. 1. Super Typhoon Dorian on December 3, 2006 from the earth observatory using data provided courtesy of the MODIS Rapid Response Team and NASA Goddard Space Flight Center by Jesse Allen (2006), Hundreds of people in Viet Nam are homeless and the families search through hundreds of destroyed villages for loved ones by Live Science (2006).

Supporting over one quarter of the Thai population, coastal regions are increasingly vulnerable to both chronic and acute hazards. Coastal zone hazards include coastline sediment and erosion (Ekphisutsuntorn et al., 2010), flooding of low-lying areas, sea level rise, and plumes of noxious algae, toxins, pollutants, pathogens, and suspended matter. How can we best forecast, assess, and respond to the environmental hazards that shape our coasts and sustain the marine and human life dependent upon coastal resources?

To date, environmental hazard monitoring in the ESS cluster, JGSEE at King Mongkut's University of Technology Thonburi, Thailand has primarily focused on Atmosphere-Ocean-Coastal-based hazards, such as coastal erosive reduction, sediment transport, morphological evolution, flood, tropical cyclone wind-wave, storm surge, strong current, heavy rainfall and their impacts on the local countries. The environmental hazards, however, have tremendous impacts on the world's oceans, the communities residing along coastlines and the economies they support. Recent years have witnessed record-breaking natural hazards impacting coastal zones. Worldwide, the number of intense Category 4 and 5 hurricanes has nearly doubled since the 1970s.

A moving tropical cyclone is an intense source of surface wind stress and sea level pressure that causes many significant changes in ocean wind-wave, storm surge and current (WSC) characteristics (Wannawong et al. 2010d). These features have been well identified in open oceans in the western Atlantic/eastern Pacific regional seas, for example, the Hurricane Region (HR). A hurricane with an intense and fast-varying wind produces a severe and complex ocean wave field that can propagate for thousands of kilometers away from the storm center, resulting in dramatic variation of the wave field in space and time (Barber & Ursell, 1948). To investigate the wave characteristics, the directional spectra of hurricane generated waves were measured using various instruments. For example, the fetch effect was detected in the Celtic Sea using the high-frequency radar. The wave characteristics of the northeast Pacific during the passage of a storm were investigated by using the synthetic aperture radar image from the ERS-1 satellite (Holt et al., 1998). The spatial wave variation of hurricane directional wave spectra were identified for both open ocean and landfall cases using the NASA scanning radar altimeter (Wright et al., 2001; Walsh et al., 1989). The directional wave spectra from the ocean surface topography were computed by Hwang and Wang (2001). The ocean wave response identified in the HR has a significant right forward quadrant bias in the significant wave height (Hs). During the passage of Hurricane Bonnie (1998) in the Atlantic Ocean, both observational and modeling studies showed that the Hs reached 14 m in the open ocean (Wright et al., 2001; Moon et al., 2003). The maximum Hs appeared in the right forward quadrant of the hurricane center and propagated in the same direction as the hurricane. Moon et al. (2003) simulated the wave characteristics successfully using the wave model such as the WAVEWATCH-III (WW3) (Tolman, 1991) and found that the hurricane-generated wave field was mostly determined by two factors: the distance from the hurricane center or radius of maximum winds (represented by Rmax) and the hurricane translation speed. For the case of a hurricane with low translation speed, the dominant wave direction is mainly determined by the distance from the hurricane center.

However, most of the observational and modeling studies on ocean waves generated by tropical cyclones were focused in the HR. A few observational and/or modeling studies have been conducted in the Typhoon Region (TR), especially in the South China Sea (SCS) and the Gulf of Thailand (GoT). The topographical information of the SCS and GoT is

shown in Fig. 2. Also due to its semi-enclosed nature, the SCS and GoT are subjected to high spatial and temporal variability from external forcing factors. One significant source of the SCS and GoT variability is the tropical cyclones that routinely affect the TR. The WW3 has been implemented and verified for the SCS using the TOPEX/POSEIDON satellite data (Chu et al., 2004). For the storm surge, an abnormal high sea level phenomenon is generated by very low pressure accompanied with very strong wind (tropical cyclone). Naturally, water can flow freely in the open sea in duration of the occurring of tropical cyclone, but not on land. Therefore, the water is piled-up at the shore and spilled over lands. This causes serious hazards to coastal regions, such as flooding, coastal erosion, etc., and devastating the residential properties in those areas. In the GoT, the tropical cyclones affecting Thailand usually take a course from the Western North Pacific Ocean or the South China Sea (SCS). The extreme of tropical cyclones is typically characterized by wind speed and a pressure drop at the eye of the storm. The GoT is subjected to the monsoon system which influences the surface currents clockwise during the southwest monsoon and counterclockwise during the northeast monsoon. The GoT is affected by tropical cyclones because of its location farther inland. However, WSC characteristics have not been well identified in the GoT. There were seven severe typhoons that previously passed through the GoT (Typhoon Vae in 1952, Tropical Storm Harriet in 1962, Typhoon Gay in 1989, Typhoon Becky in 1990, Typhoon Fred in 1991, Typhoon Forrest in 1992 and Typhoon Linda in 1997). The occurring

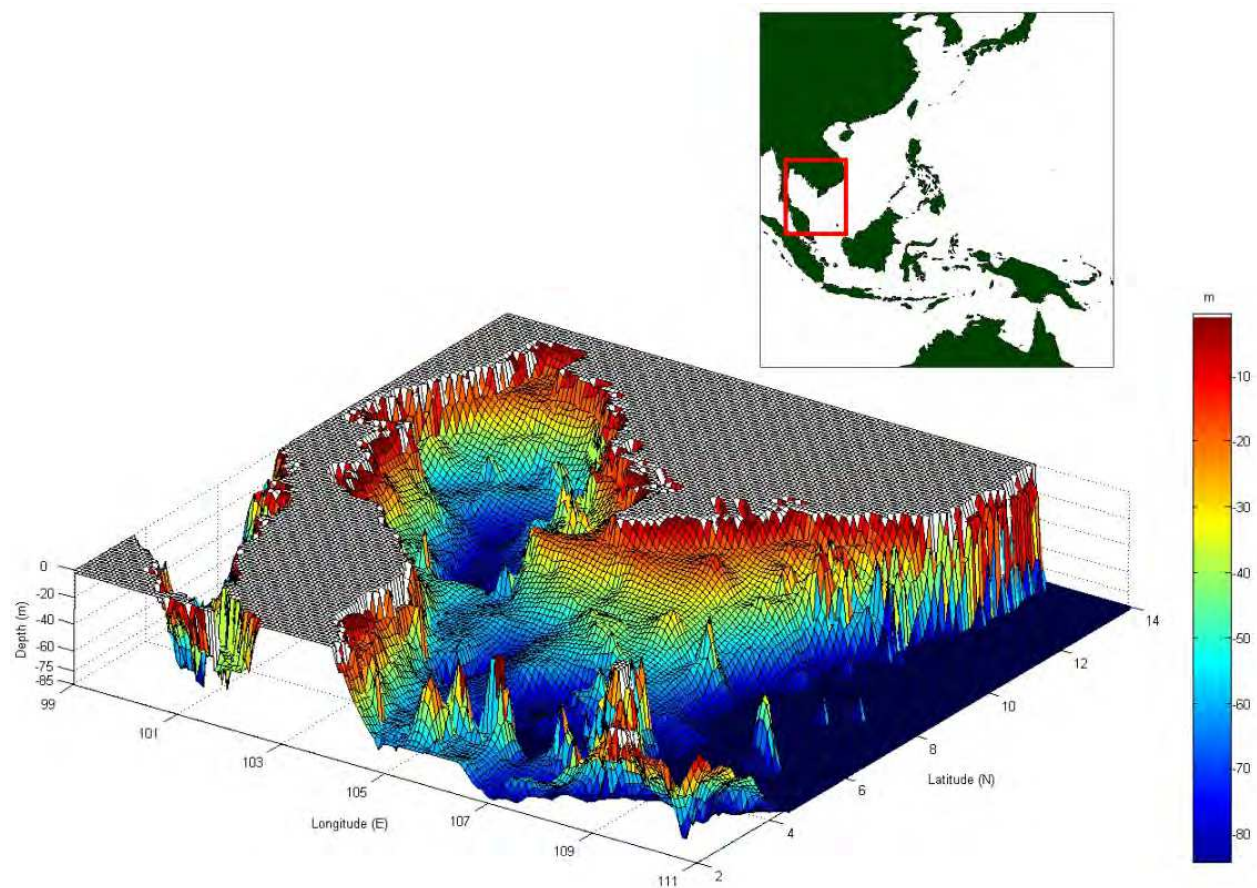


Fig. 2. Bathymetry in a three dimensional perspective with depth (in meters)

frequency of the tropical cyclone is approximately once in every two years and some can cause severe damage to lives and properties in the coastal area. For example, in 1962, Tropical storm Harriet hit Leam Talumpuk, NakornSriThammarat province and caused severe damages to the area including more than 900 casualties. In 1989, Typhoon Gay hit Chumporn province causing serious disaster, such as destroying the agricultural lands (about 183,000 hectare (ha) or 1.83×10^9 m²), killing over 400 people, and directly affecting 154,000 people. In 1997, Typhoon Linda struck at Thupsake, PrachuapKirikhan province, resulting in 30 people death, 102 people missing, and more than 400,000 Rai (6.4×10^8 m²) of agricultural land destroyed. Therefore, the warning WSC system is needed for people who live in risking regional and coastal areas. At present, there is no such the favorable warning of WSC system for the regional and coastal regions in Thailand. This chapter was to examine how WSC affects the regional and coastal areas in the SCS and GoT, and to modify the meteorological models to predict the WSC characterized by tropical cyclones in the SCS and GoT. In this chapter, Typhoon Linda in 1997 was firstly studied to serve as inputs in the meteorological model predictions and useful in the test cases of Typhoon Muifa in 2004 and Typhoon Durian in 2006 respectively.

2. Methodology

The methods and steps to study the cyclone WSC characteristics in the SCS were described in this section. The cyclones generated and entering the study domain (Fig. 2) were chosen according to the statistical data obtained from the Joint Typhoon Warning Center (JTWC) and the Thai Meteorological Department (TMD). The meteorological prediction models were applied to simulate WSC as considered under the statistical data which presented in Section 2.1. The histories of three typhoons were given in Section 2.2. The model description was described in Section 2.3. Finally, the model setting and implementation were explained in Section 2.4.

2.1 Statistical data of tropical cyclone

The yearly statistical data in 1951 to 2009 of the TMD were reported that there were only 3 severe tropical cyclones generated in the GoT: Typhoon Vae in 1952, Super Typhoon Gay in 1989 and Typhoon Linda in 1997. Typhoon Gay was classified as the category 1 in the GoT. It then made landfall in the southern part of Thailand and upgraded to the categories 2 and 3. It began to weaken slightly (category 1) as it moved out of Thailand. It upgraded back to the category 5 as it approached land in India. Typhoon Linda behaved as the category 1 in the GoT. It was influenced by Super Typhoon Keith (category 5) entering the Pacific Ocean nearby the Philippine Islands and also the local wind. In term of numbers of tropical cyclone, 18 tropical cyclones were the maximum number reported in 1964 to 1965. They were classified as 17 tropical depressions and 1 tropical storm. According to the statistical data, it was found that the numbers of tropical cyclone decreased since 1965 to 2009 as shown in Fig. 3.

The yearly statistical data in 1951 to 2009 considered as monthly data were found that the tropical cyclone was not found during January to March. The maximum number of tropical cyclone was reported in October with totally 51 tropical cyclones. They were classified as 47 tropical depressions, 3 tropical storms and 1 severe tropical cyclone which were Typhoon Vae in October 1952. In November, 2 severe tropical cyclones which were Super Typhoon

Gay in 1989 and Typhoon Linda in 1997 were reported as presented in Fig. 4. The third highest numbers of tropical storm were found in September, October and November with the percentages of 26, 28 and 16% respectively. Thus, the data suggest that the severe tropical cyclones in Thailand generally found as the winter storm (Fig. 5). From the statistical data, the characterizations of three severe winter storms: Typhoon Muifa 2004 (category 4), Super Typhoon Durian 2006 (category 5) as well as Typhoon Linda in 1997 (category 1) entering our study domain were studied as illustrated in Fig. 6.

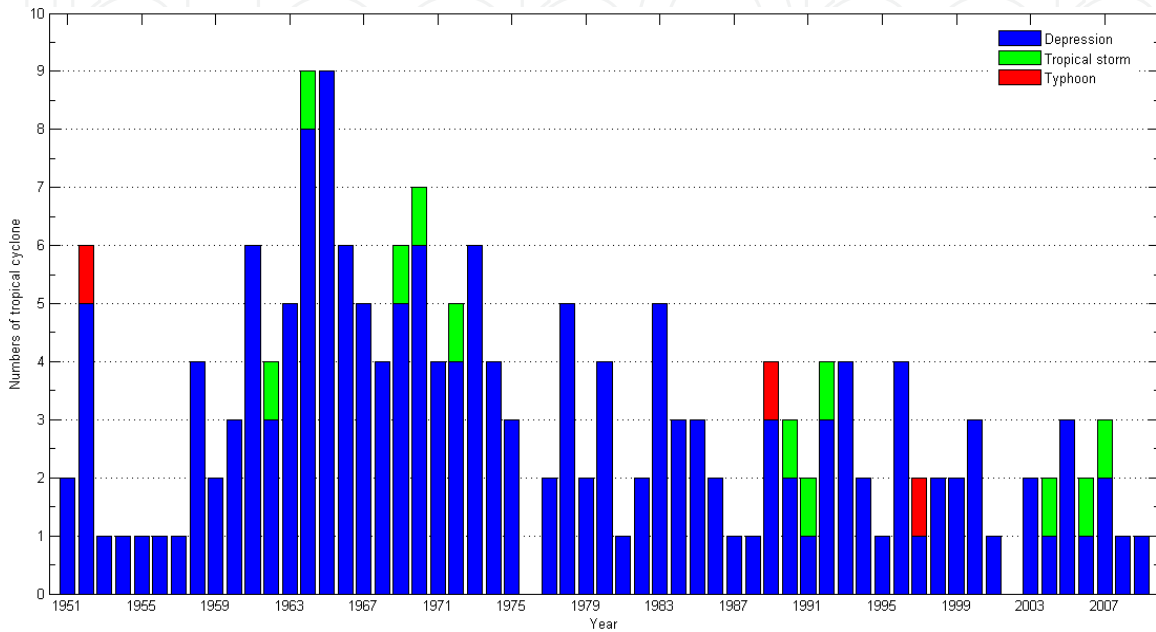


Fig. 3. Numbers of tropical cyclone passing the SCS, Thailand and entering the study domain in 1951–2009

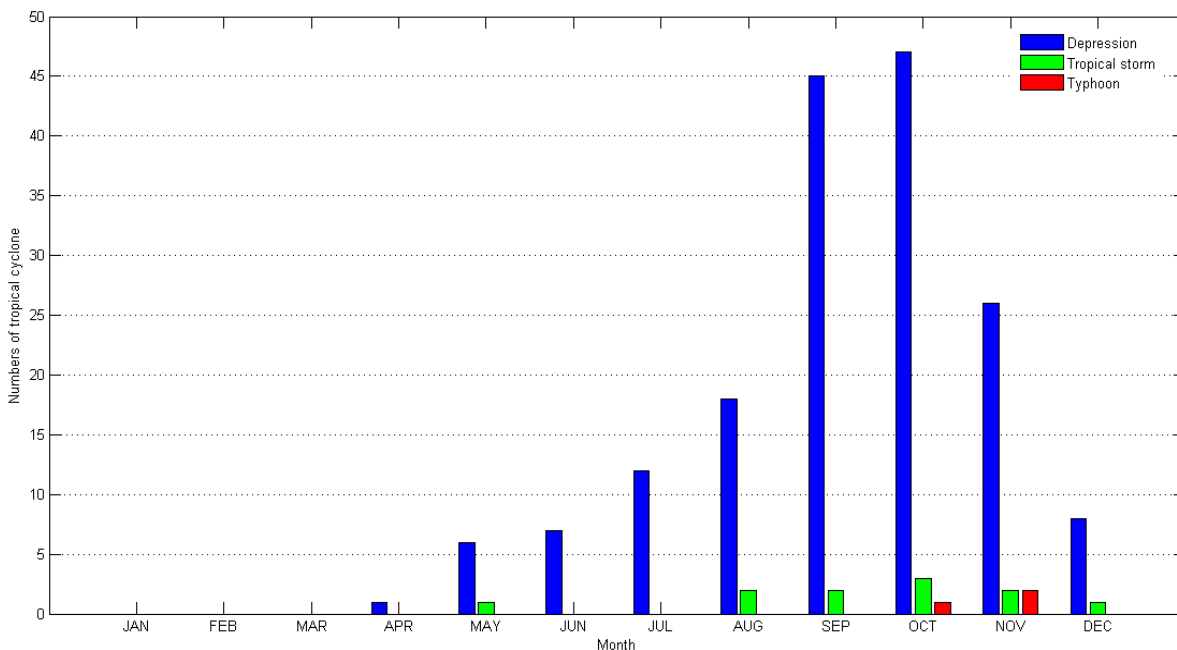


Fig. 4. Numbers of tropical cyclone passing the SCS, Thailand and entering the study domain during January–December in 1951–2009

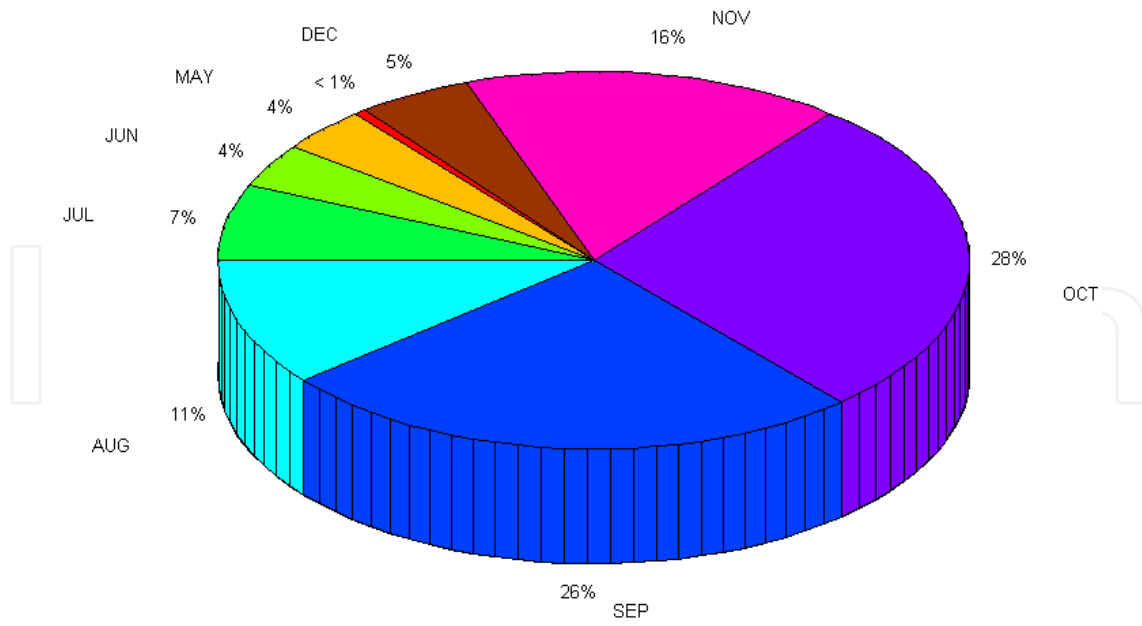


Fig. 5. Percentages of numbers of the tropical cyclone passing the SCS, Thailand and Entering the study domain during January-December in 1951 -2009

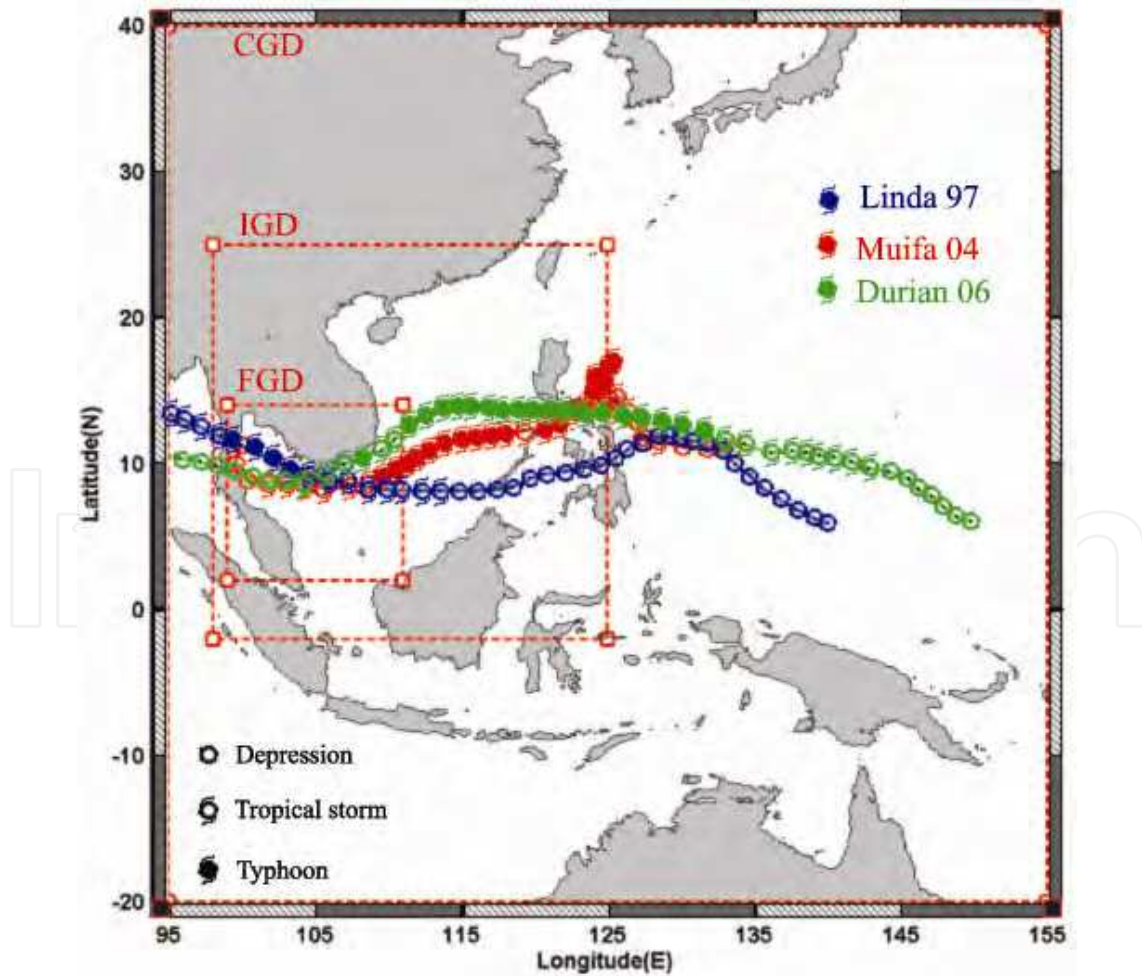


Fig. 6. Three steps of the standard one-way nested grid with Typhoon tracks

2.2 History of tropical cyclone

Typhoon Linda formed as the tropical disturbance on October 26, 1997 within an area of convection east of the Philippine Islands which is near 130°E in longitude and 10°N in latitude. It then moved westward under the subtropical ridge to the north. When entering the SCS, Typhoon Linda transformed into a tropical storm and moved westward to the southern tip of Cape Camau of Vietnam at 0900 UTC on 2 November with the intensity of 55 knots (28 m s^{-1}). After that, it approached the GoT around 00.30 UTC on 3 November with typhoon intensity in a range of 64-82 knots (approximately $33\text{-}42 \text{ m s}^{-1}$) (Fig. 7) and turned northwestward following steering from the subtropical ridge. Its strength weakened as it encountered mountains in Prachaubkirekhun province, Thailand. After crossing over the Andaman Sea, it reconsolidated and became typhoon once again at 00.00 UTC on 6 November.

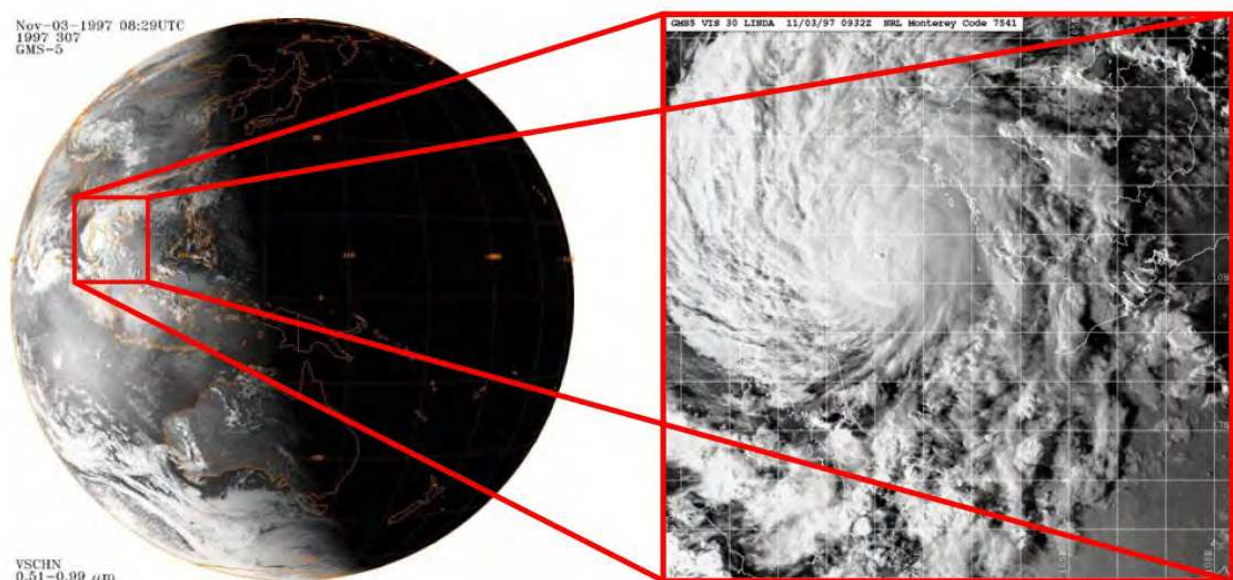


Fig. 7. GMS-5 visible images of Typhoon Linda at 08.29 UTC and 09.32 UTC on November 3, 1997 when it located at center of the GoT.

Typhoon Muifa generated as a tropical depression on 11 November 2004 in the Western North Pacific Ocean. It moved steadily northwestward through north of Palau before entering the Philippine Sea. It was firstly mentioned by the JTWC at 16.00 UTC on 13 November, approximately 400 km north of Palau. It became a tropical storm on 14 November and was named as Muifa by the Japan Meteorological Agency (JMA). On 18 November, the intensity of Typhoon Muifa was peaked at 115 knots (54 m s^{-1}). It went west-southwestwards across the SCS and its intensity reached the second peak of 90 knots (46.3 m s^{-1}) at 18.00UTC, approximately 800 km east of Vietnam. Typhoon Muifa entered Vietnam on 22-23 November and weakened again. The maximum velocity was further decreased to 45 knots (23.2 m s^{-1}) at 12.00 UTC on 24 November. Typhoon Muifa continuously weakened to 30 knots (15.4 m s^{-1}) and downgraded to tropical depression at 12.00 UTC on 25 November. At 00.00UTC on 26 November, its final position was 250 km south-southwest of Bangkok, Thailand.

Typhoon Durian was designated as a tropical depression on 25 November. It then was upgraded to a tropical storm at 06.00UTC on 26 November. It intensified slowly and moved west to west-northwestward with the intensity of 35 knots (18 m s^{-1}). Then it was intensified to 50 knots (25.7 m s^{-1}) on 27 November and became a severe tropical storm. On November 28, it continued to track towards the Philippines. Rapid intensification occurred on November 29, causing the JMA to upgrade the storm to 100 knots (51.4 m s^{-1}) in wind intensity. It began to weaken slightly as it approached land but quickly regained peak strength. It made landfall on 30 November over southern Catanduanes. It then made another landfall after crossing the Lagonoy Gulf in northeastern Camarines Sur. It finally moved to the SCS and made landfall in Ben Tre Province, Vietnam on 5 December with the decreased intensities from 55 to 25 knots (28.3 to 12.9 m s^{-1}). It rapidly weakened over land, and it was downgraded to a tropical storm by JMA.

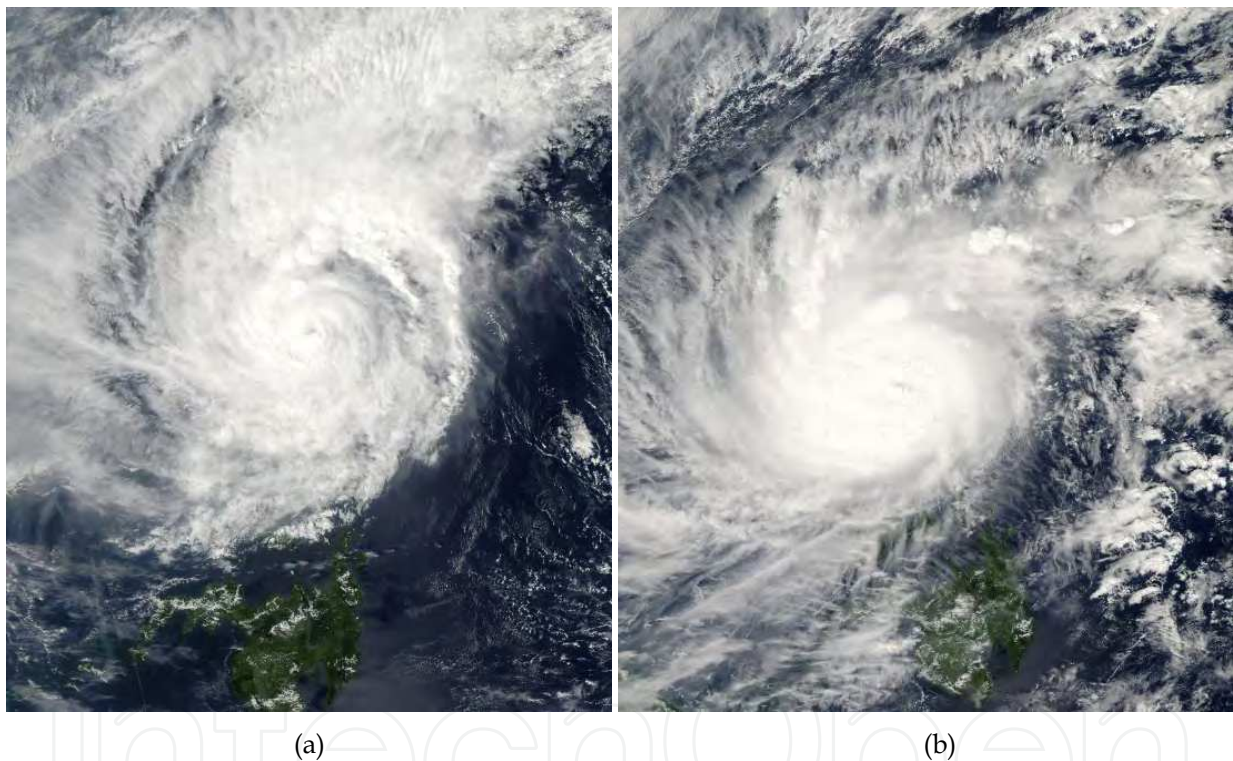


Fig. 8. MODIS-Aqua 250 m imagery of Typhoon Muifa (a) and Super Typhoon Durian (b) at 04.55 UTC on November 17, 2004 and at 05.00 UTC on November 30, 2006, respectively.

2.3 Model description

The wind-wave model is based on the Wave Model Cycle 4 (WAMC4) to simulate the surface wave (WAMDI Group, 1988; Komen et al., 1994) and the hydrodynamic model is based on the POM model including the storm surge and current modeling components to simulate the storm surges and current fields (Blumberg and Mellor, 1987). Both models were used to simulate the impacts of Typhoon Linda 1997, Typhoon Muifa 2004 and Super Typhoon Durian 2006 in the meteorological prediction. This section briefly described the information of WSC models.

2.3.1 Wind-wave model

In the absence of diffraction and currents, the spectral energy balance equation which is the basic equation of spectral wave model in Cartesian coordinates, is (e.g., Komen et al., 1994)

$$\frac{\partial E}{\partial t} + \frac{\partial(c_x E)}{\partial x} + \frac{\partial(c_y E)}{\partial y} + \frac{\partial(c_\theta E)}{\partial \theta} = S_{tot} \quad (1)$$

where $E(t, x, f, \theta)$ is the energy density of wave, t is the time, x is the Cartesian coordinates that are geographical space (x, y), f is the frequency, θ is the wave direction measured clockwise from the true north, c_x and c_y are the propagation velocities of the group velocity c_g in geographical space and c_θ is the propagation velocity in spectral space (directional space). These propagation speeds are taken from the linear theory of surface gravity waves without the effects of diffraction. The governing equation for the WAMC4 model (Eq. 1) in the spherical coordinates reads (WAMDI Group, 1988),

$$\frac{\partial E}{\partial t} + \frac{\partial(c_\lambda E)}{\partial \lambda} + (\cos \phi)^{-1} \frac{\partial(c_\phi \cos \phi E)}{\partial \phi} + \frac{\partial(c_\theta E)}{\partial \theta} = S_{tot} \quad (2)$$

where $E(t, x, f, \theta)$ is the energy density of waves, x is the spherical coordinates that are geographical space (λ, ϕ), c_λ and c_ϕ are the propagation velocities of the group velocity c_g in the geographical space and c_θ is the propagation velocity in the spectral space. The left-hand side of Eqs. (1)-(2) is the regional scale (e.g. GoT). It represents the local rate of change of wave energy density in time, propagation in geographical space, and shifting of frequency and refraction due to the spatial variation of the depth and current. The right-hand side of both equations (S_{tot}) shows all effects of generation and dissipation of the waves in deep water including wind input (S_m), white capping in dissipation (S_{ds}) and non-linear quadruplet wave-wave interactions (S_{nl}) in deep water. These equations, however, ignored the current interactions in this study. In shallow water, both equations need to be extended to include an additional source function (S_{bf}) representing the energy loss due to bottom friction and percolation. The bottom friction dissipation term (S_{bf}) represented the formulation proposed during JONSWAP (Hasselmann et al., 1973),

$$S_{bf} = -\frac{\Gamma}{g^2} \frac{\omega^2}{\sinh^2 kD} E \quad (3)$$

with $\Gamma = 0.038$, ω is the angular frequency ($\omega^2 = gk \tanh kD$), g is the gravitational acceleration, k is the wave number and D is the finite depth dispersion relation.

2.3.2 Storm surge and current model

The Princeton Ocean Model (POM) is based on the hydrodynamic model which is a three-dimensional, nonlinear, primitive equation with the finite difference ocean model (Blumberg and Mellor, 1987). The POM model uses a mode-splitting technique that solves the barotropic mode (2D) for the free surface and vertically averaged horizontal currents, and the baroclinic mode (3D) for the fully three-dimensional temperature, turbulence, and current structure. The equations are written in the sigma vertical coordinate system and

include a turbulence closure parameterization with an implicit time scheme for vertical mixing. These are the vertically integrated nonlinear continuity and horizontal momentum equations, which solve the water level and the horizontal components of velocity (u, v). In the present work, these equations were modified by the storm surge applications to simulate the storm surges and currents in the 2D and 3D modes respectively. At the sea surface boundary, the model was forced by wind stress and atmospheric pressure of Typhoon Linda, whereas tidal forcing, current and river outflow at the lateral boundary conditions were not considered. The typhoon pressure field and surface wind velocity created by the pressure gradient were modeled following the Bowden (1983) and Pugh (1987) relationships:

$$\frac{\partial p_a}{\partial \eta} = -\rho g, \quad (4)$$

$$\frac{\partial \eta}{\partial x} = \frac{\rho_a C_d V_c^2}{\rho g d}, \quad (5)$$

where p_a is the atmospheric pressure, η is the sea surface elevation from the reference level of undisturbed surface, ρ is the density of sea water, g is the gravitational acceleration of Earth, x is the coordinate in the east-west direction, ρ_a is the density of air, C_d is the drag coefficient, V_c is the wind profile that results from the typhoon pressure gradient and d is the depth of sea water. According to Eq. (4), the pressure decreasing for 1 mb corresponds to about a 1 cm rise in sea level. The water depth (d) has inversely affected the sea surface elevation (η), whereas the wind speed at the specific height (10 m) directly affects the sea surface elevation.

The wind stress is computed through the following bulk formula:

$$\tau = \rho_a C_d |\bar{V}_w| \bar{V}_w, \quad (6)$$

where V_w is wind speed at height of 10 m, ρ_a is the density of air, and the drag coefficient, C_d , is assumed to vary with wind speed as:

$$10^3 C_d = \begin{cases} 2.5 & \text{if } |\bar{V}_w| > 22 \text{ m s}^{-1} \\ 0.49 + 0.065 |\bar{V}_w| & \text{if } 8 \leq |\bar{V}_w| \leq 22 \text{ m s}^{-1} \\ 1.2 & \text{if } 4 \leq |\bar{V}_w| < 8 \text{ m s}^{-1} \\ 1.1 & \text{if } 1 \leq |\bar{V}_w| < 4 \text{ m s}^{-1} \\ 2.6 & \text{if } |\bar{V}_w| < 1 \text{ m s}^{-1} \\ 0.63 + 0.066 |\bar{V}_w| & \text{for all } |\bar{V}_w| \\ 0.63 + \left(0.066 |\bar{V}_w|^2\right)^{1/2} & \text{for all } |\bar{V}_w|. \end{cases}$$

This C_d formula follows Large and Pond (1981) when the wind speed is less than 22 m s^{-1} , otherwise, it is assumed as a constant as indicated in Powell et al. (2003). In the present study, the last condition was selected. The horizontal momentum equations consist of local time derivative and horizontal advection terms, Coriolis deflection, sea level pressure gradient, tangential wind stress on the sea surface, and quadratic bottom friction. The system of equations is written in flux form and solved using a finite differencing scheme that is centered in time and space on the Arakawa C grid.

2.4 Model setting and Implementation

The operational WSC model system contained three domains, which covered the Pacific Ocean, SCS and GoT (Fig. 6), in order to study the impacts of strong WSC generated by Typhoon Linda, Typhoon Muifa and Super Typhoon Durian.

The wind-wave (WAMC4) model required the topographical data and input wind fields to be specified for each grid cell in each grid domain. The topographical data was obtained from ETOPO5, ETOPO1 and Royal Thai Navy (Amante and Eakins 2008; Edwards 1989; Wannawong et al. 2010a). The ETOPO5 was updated in June 2005 for deep water conditions and it was applied in the CGD in this study. The ETOPO1 (Bedrock version) was applied in both IGD and FGD. The bathymetry data obtained from the Royal Thai Navy was only applied to the FGD which is shown in Fig. 9. The merging of the Royal Thai Navy data, ETOPO1 and ETOPO5 data, and the nested grid method were described in the previous studies (Wannawong et al. 2010a; Wannawong et al. 2010b; Wannawong et al. 2010c; Wannawong et al. 2010d; Wannawong et al. 2011b). The wind fields at 10-meter height were obtained from the U.S. Navy Global Atmospheric Prediction System (NOGAPS) model with 1×1 degree data resolution. Linear interpolation was used to generate the wind data to the grid points (Hogan and Rosmond 1991). The CGD covering the Pacific Ocean with the closed boundary condition was applied with a resolution of 0.5 degrees. The domain covered the area of storm generation from 95°E to 155°E in longitude and from 20°S to 40°N in latitude, which gives 121×121 grid points for both latitude and longitude. The IGD covering the SCS with the open sea condition has a resolution of 0.375 degrees. It covers from 98°E to 125°E in longitude and from 2°S to 25°N in latitude, which gives 109×109 grid points for both latitude and longitude. Finally, the FGD with open sea condition in the GoT was set to 0.25 degrees resolution. The FGD covers from 99°E to 111°E in longitude and from 2°N to 14°N in latitude, which gives 49×49 grid points for both latitude and longitude. Both propagation and source time steps of CGD, FGD and IGD were set to 1800, 1200 and 600 s, respectively (Wannawong et al. 2011c).

The storm surge and current (POM) model required the input bathymetry data, atmospheric forcing (wind and pressure fields), temperature and salinity at each grid point (Wannawong et al. 2008). The bathymetry data was taken by merging of the Royal Thai Navy data, ETOPO1 and ETOPO5 data. The wind and pressure fields were obtained from NOGAPS with 1×1 degree data resolution (Hogan and Rosmond, 1991; Harr et al., 1992). The temperature and salinity with 1×1 degree data resolution provided by Levitus94 (Levitus and Boyer, 1994; Levitus et al., 1994) were indicated by the climatological monthly mean fields in the model. The domain covered from 99°E to 111°E and 2°N to 14°N with high resolution of 0.1×0.1 degree spatial grid size which gave 121×121 points by using the bilinear interpolation of these data in the horizontal coordinate. In the vertical coordinate, 21

sigma levels were employed for adequacy and computational efficiency. The nested grids were not included in this model version. The model integration was divided into spinup and simulation phases. The model was integrated with all three components of velocity initially set to zero in the spinup phase of the model run. The model time steps were 20 s and 1200 s (20 min) for the external and internal time steps respectively (Wannawong et al. 2010d; Wannawong et al. 2010e; Wannawong et al. 2011a, Wannawong et al. 2011c). Finally, the results of both models were presented in every hour of Typhoon Linda, Typhoon Muifa and Super Typhoon Durian passing through the GoT. The simulation was started at 00UTC on October 20 and ended at 00UTC on November 10, 1997 for Typhoon Linda. In Typhoon Muifa, the simulation was performed from 00UTC on November 10 to 00UTC on November 28, 2004. Finally, the simulation was started at 00UTC on November 21 and ended at 00UTC on December 9, 2006 for Super Typhoon Durian. The results of the both models were stored every hour for the duration of the simulation. The stability of both models was computed according to the Courant–Friedrichs–Lewy (CFL) stability condition.

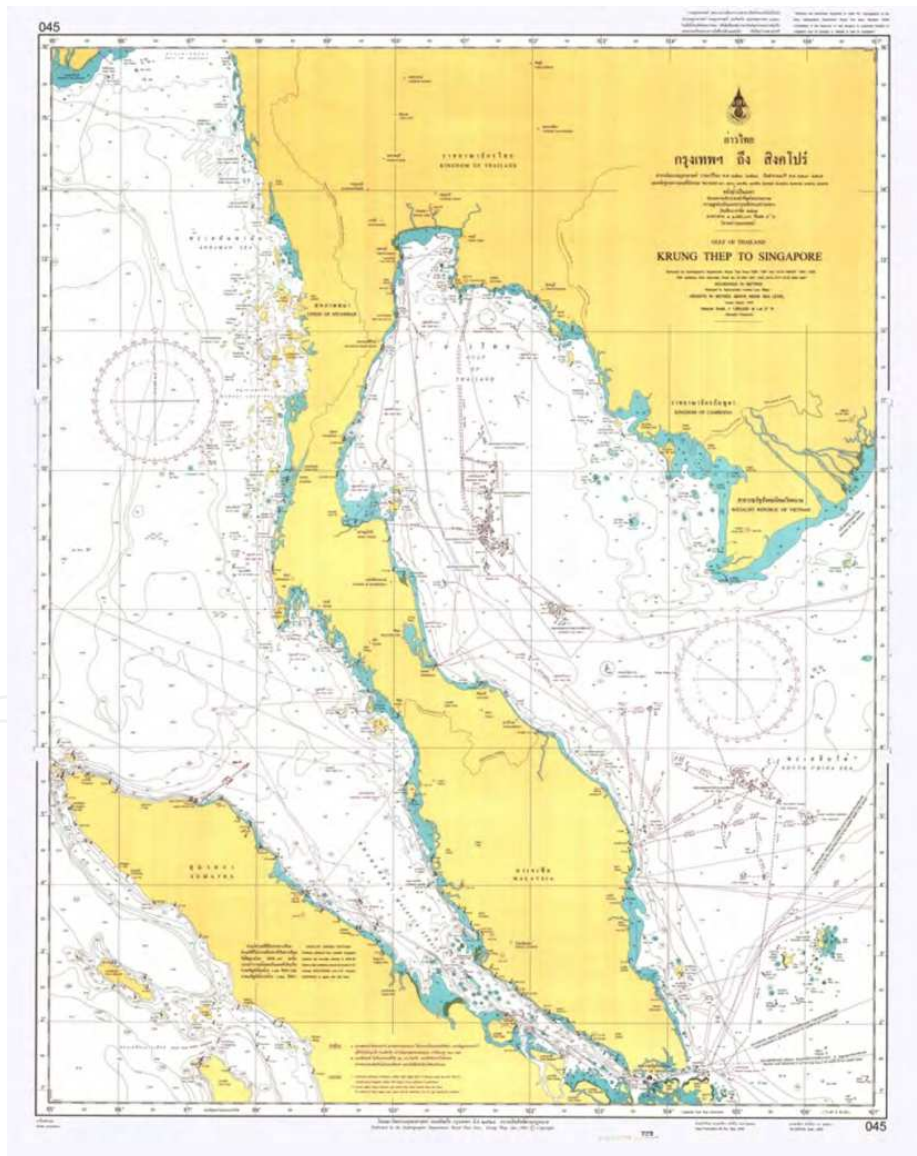


Fig. 9. Bathymetry data (annotated excerpt from the Royal Thai Navy).

3. Meteorological prediction results

The meteorological predictions of wind-wave and coordinate propagation with the flag condition of the WAMC4 model, and the storm surge and current of the POM model in the barotropic and baroclinic modes were analyzed. The meteorological predictions of the WSC generated by Typhoon Linda were firstly considered. The H_s , storm surge and current related with the wind field and sea level pressure during the passage of Typhoon Linda in each domain is shown in Figs. (11)-(12). In the CGD, Super Typhoon Keith 1997 was also found in the Pacific Ocean while Typhoon Linda was in the SCS (Fig. 11). Along the best track (Fig. 6), the FGD presented the wind field, wind stress and pressure drop related with the H_s , sea surface elevation and current (Figs. (11)-(12)). The meteorological predictions did not only present the H_s , peak surge and current but also showed the coastal water level drop and the energy loss of waves due to the bottom friction and percolation in the coastal zone (Figs. (11)-(12)). The effects of the extreme H_s , sea surface elevation and current, and the difference between the maximum H_s , sea surface elevation and current computed by the WAMC4 and POM models at four locations of buoy (B1-B4) and ten locations of tide gauges station (S1- S10) in the GoT region (Fig 10) were calculated. The results of the WAMC4 model showed that the H_s at B1, B2 and B3 were similarly different while at the station B4 showed a markedly different (H_s). The results of the POM model showed that the maximum storm surge and current at each station presented the similar values and also showed the similar trends with the observational data, except those of the stations S5, S6 and S8.

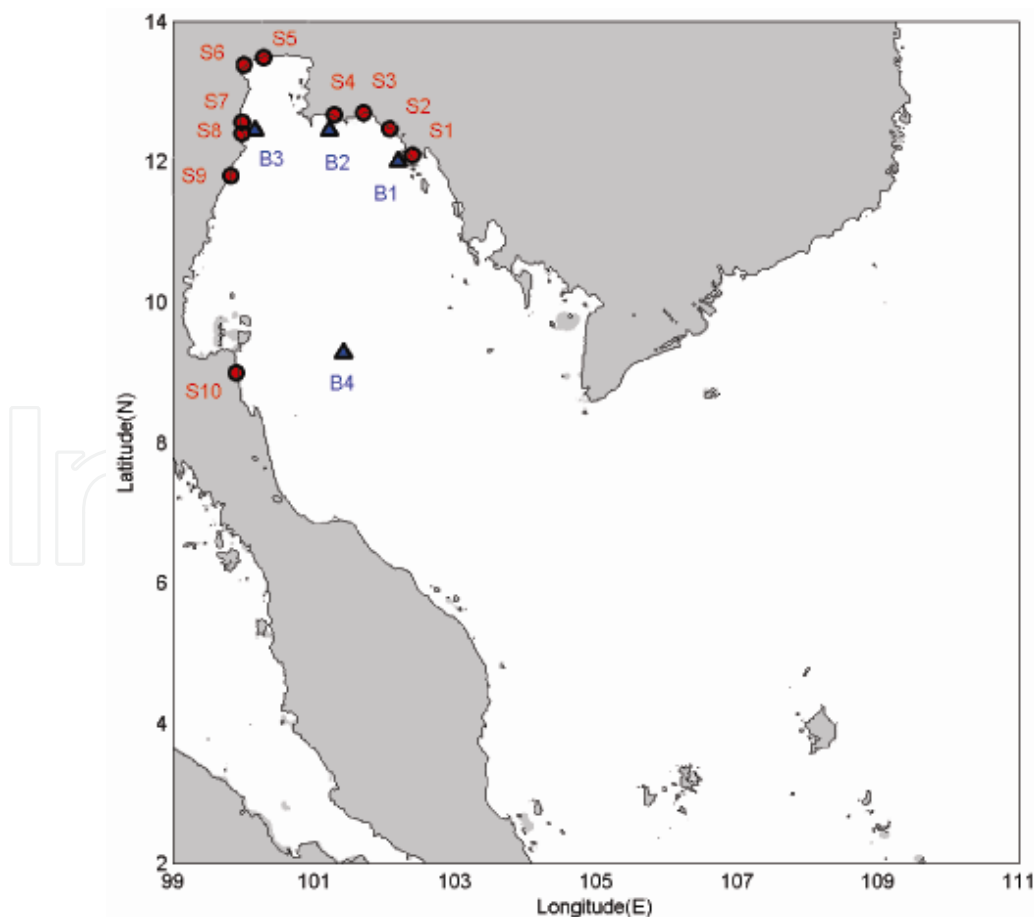


Fig. 10. Position of the observational data at each station inside the FGD

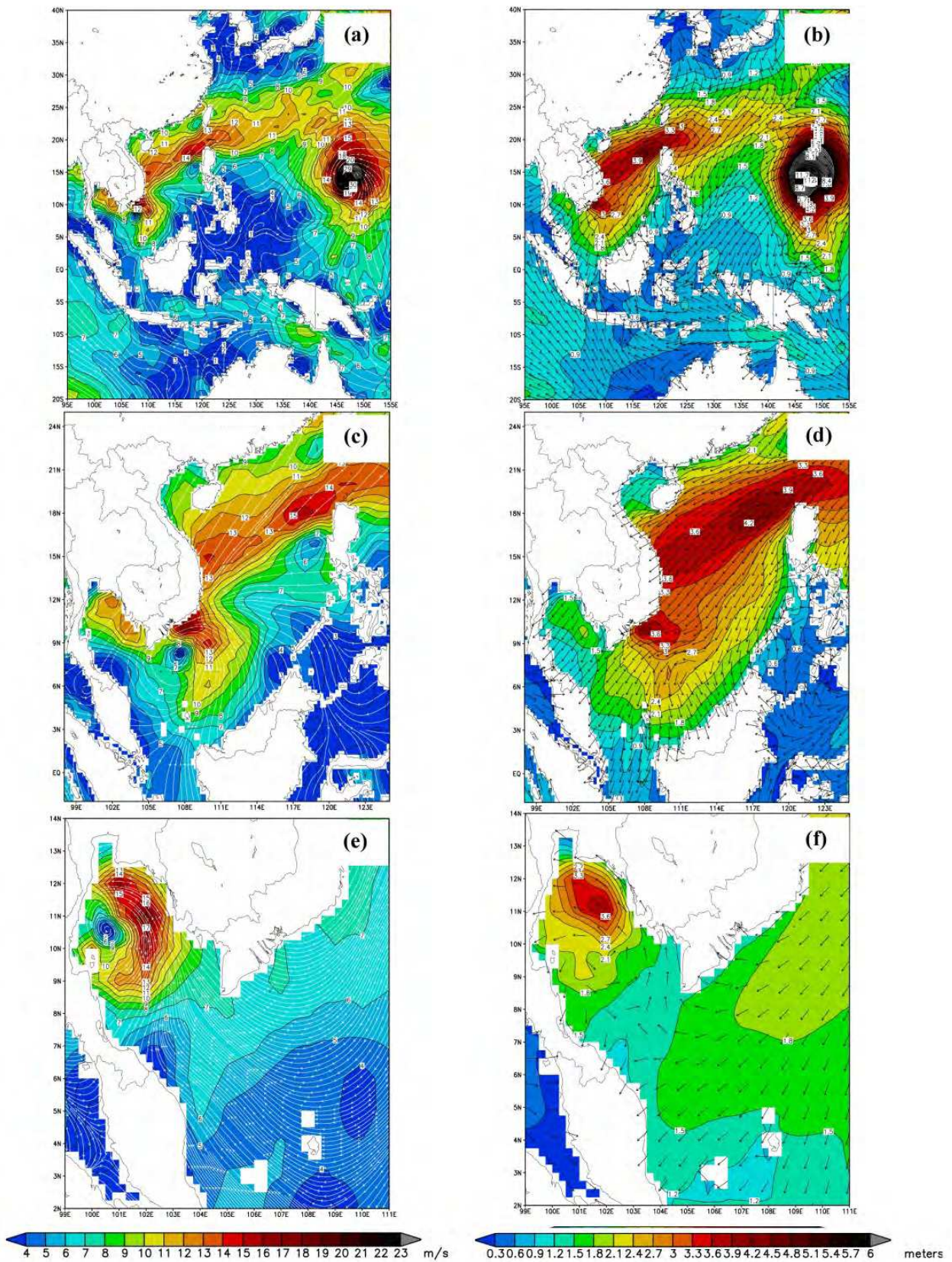


Fig. 11. Three pathway nested grids of wind streamline and speed (m s^{-1}), H_s (m) and its direction at (a) 23UTC01NOV1997, (b) 23UTC01NOV1997 and (c) 12UTC03NOV1997 in the CGD, IGD and FGD

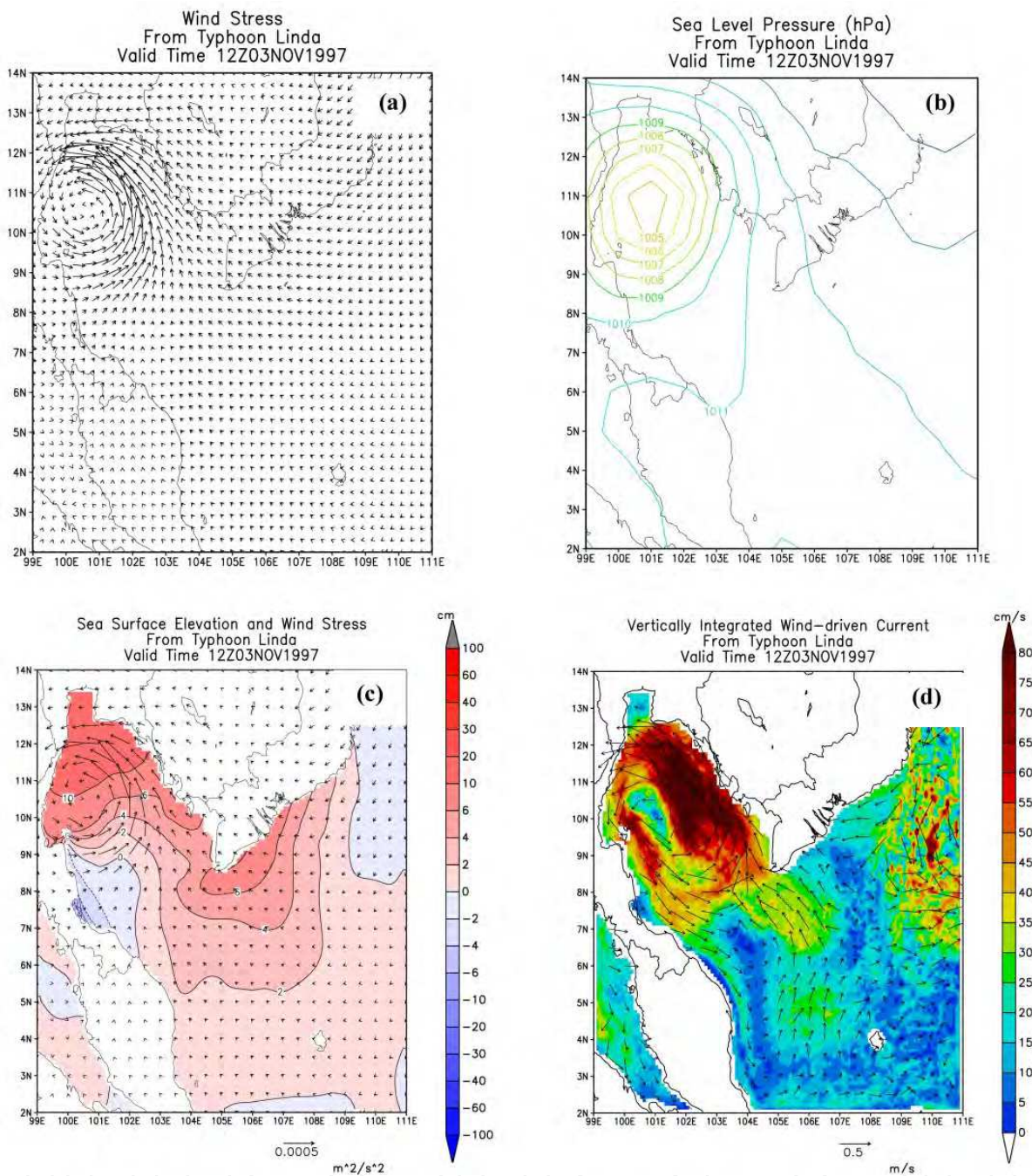


Fig. 12. (a) Wind stress (m^2s^{-2}), (b) Sea level pressure (hPa), (c) Sea surface elevation (cm) and wind stress (m^2s^{-2}), (d) current ($cm s^{-1}$) and its directions at 12UTC03NOV1997 in the FGD

The H_s , storm surge and current related with the wind field and sea level pressure during the passage of Typhoon Muifa and Super Typhoon Durian only in FGD domain is shown in Figs. (13)–(18). Along the best track (Fig. 6), the FGD presented the wind field, wind stress and pressure drop related with the H_s , sea surface elevation and current (Figs. (13)–(18)). The meteorological predictions also present the H_s , peak surge and current with the coastal water level drop and the energy loss of waves due to the bottom friction and percolation in the coastal zone (Figs. (13)–(18)).

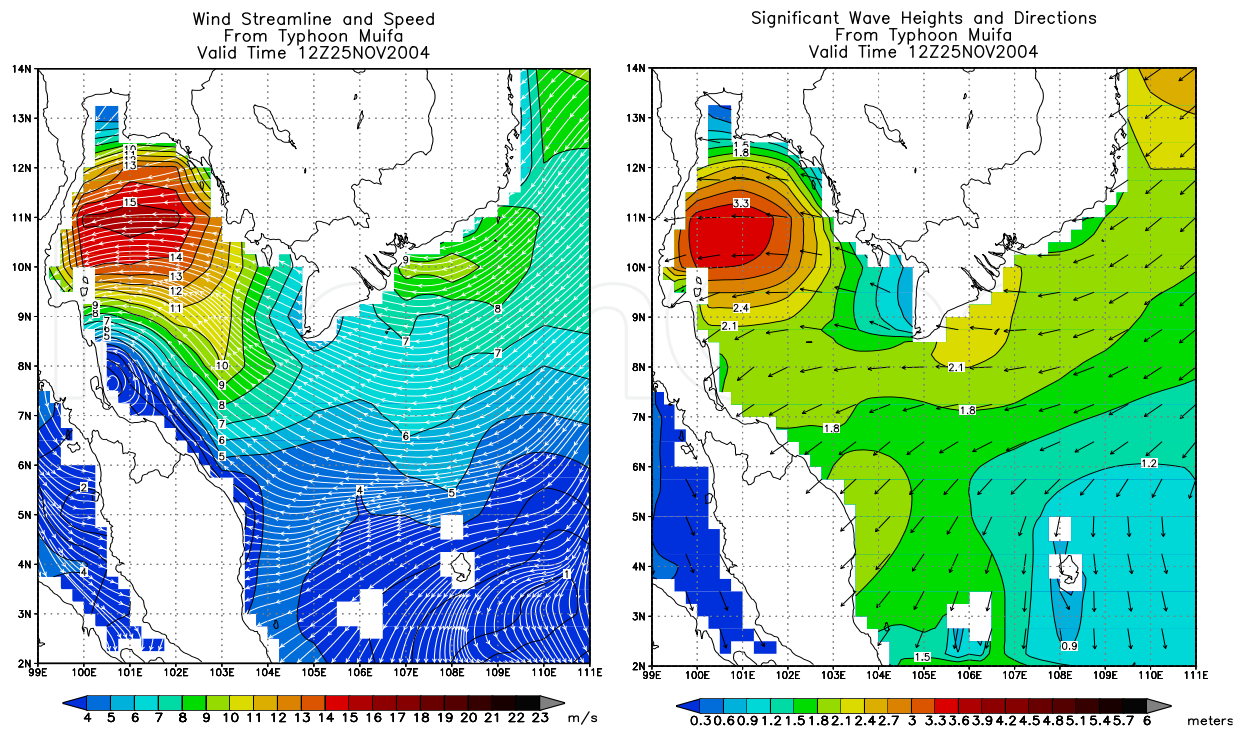


Fig. 13. (a) Wind streamline and speed ($m s^{-1}$) and (b) H_s (m) and its direction at 12UTC25NOV2004 in the FGD

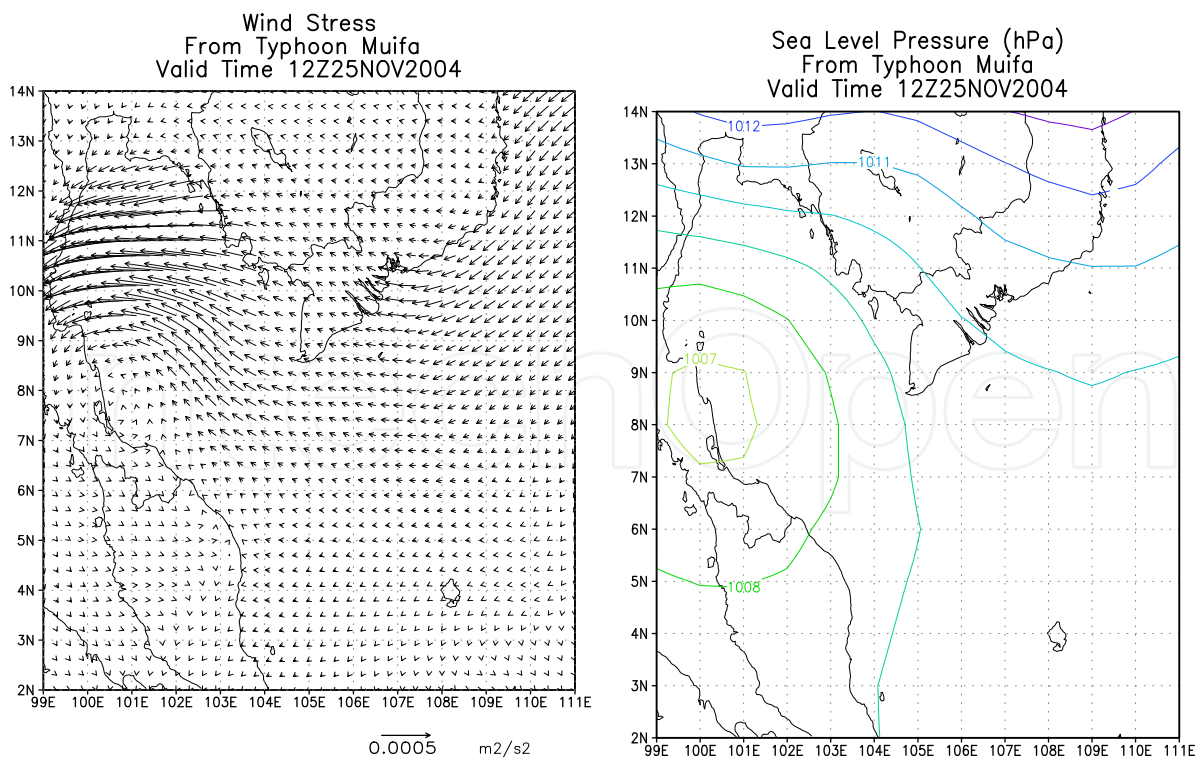


Fig. 14. (a) Wind stress ($m^2 s^{-2}$) and (b) Sea level pressure (hPa) at 12UTC25NOV2004 in the FGD

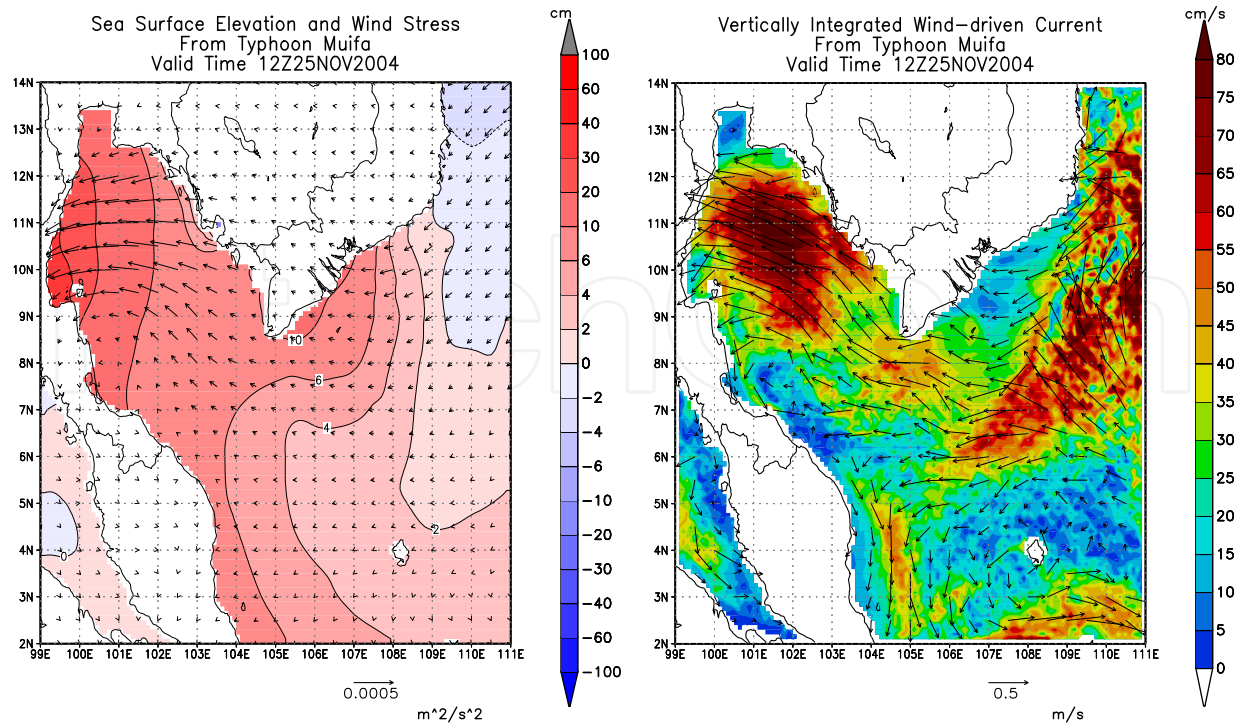


Fig. 15. (a) Sea surface elevation (cm) and wind stress ($m^2 s^{-2}$) ; (b) current ($cm s^{-1}$) and its directions at 12UTC25NOV2004 in the FGD

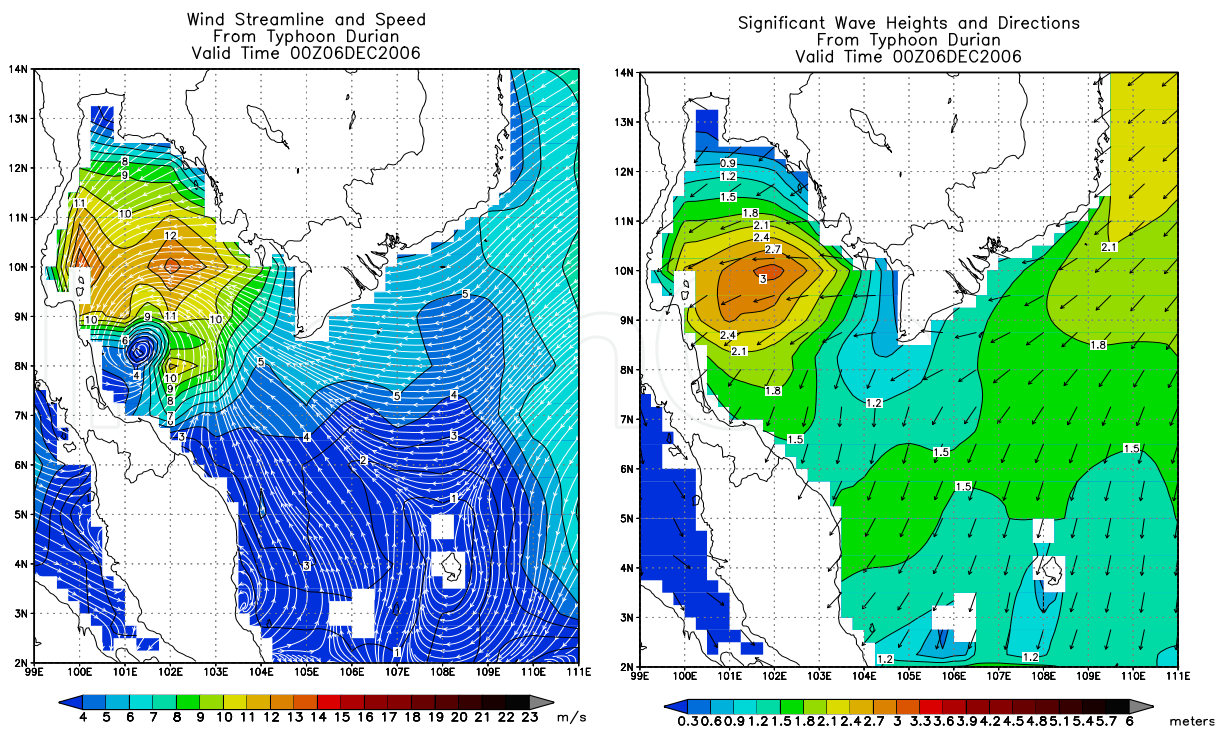


Fig. 16. (a) Wind streamline and speed ($m s^{-1}$) and (b) H_s (m) and its direction at 00UTC06DEC2006 in the FGD

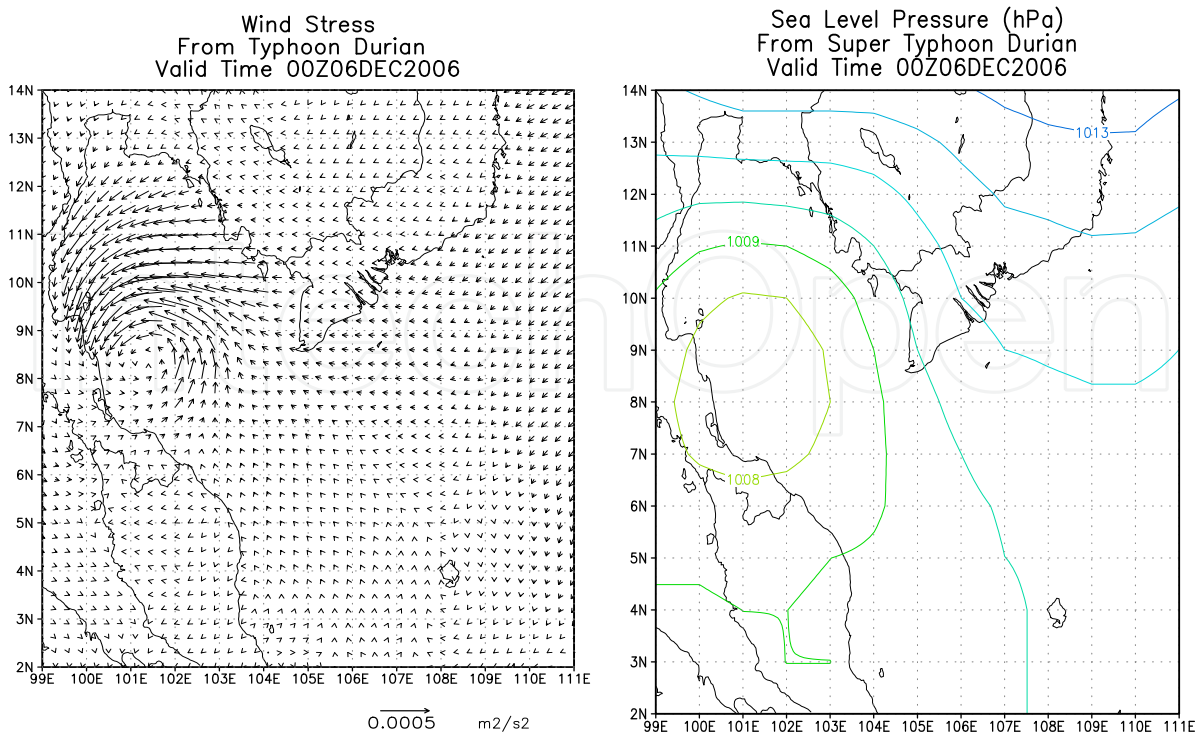


Fig. 17. (a) Wind stress ($\text{m}^2 \text{s}^{-2}$) and (b) Sea level pressure (hPa) at 00UTC06DEC2006 in the FGD

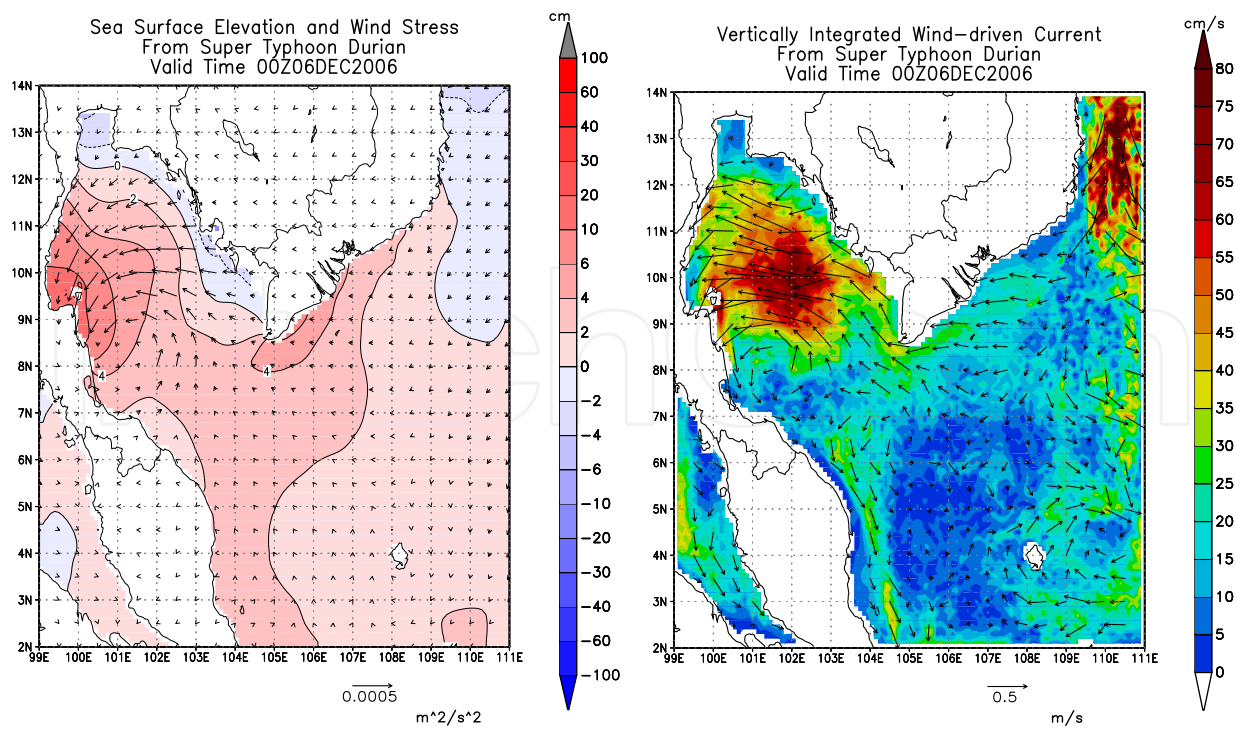


Fig. 18. (a) Sea surface elevation (cm) and wind stress ($\text{m}^2 \text{s}^{-2}$); (b) current (cm s^{-1}) and its directions at 00UTC06DEC2006 in the FGD

4. Discussion and conclusion

The results of both models are presented the incorporated Hs in the regional zone affects into the coastal storm surge zone. Specifically, the results are indicated that the WSC generally under the approximation is not only the peak surge but also the coastal water level drop which can also cause substantial impact on the coastal environment. The wind and sea level pressure fields induced the storm surge and current can significantly improve storm surge and current in the meteorological prediction. The both model system can be particularly useful to study wind-induced the WSC. The WSC in this study demonstrate the impact of severe storms in the GoT. The results indicate that Typhoon Linda was the most severe storm in 21 years according to data collected by the Joint Typhoon Warning Center (JTWC) and the Thai Meteorological Department (TMD). It can be explained that the passage of Super Typhoon Keith (1997) into the SCS led to the upgrading of Typhoon Linda from tropical storm to a category 1 typhoon. On the other hand, Typhoon Muifa and Super Typhoon Durian weakened when they approached the GoT and they were downgraded to tropical storms. Their wind intensities continuously decreased leading to decreasing the WSC. This is because the southern part of Vietnam is abundant in forests which act as natural walls to protect Thailand from storms and heat supplied from the warm sea. In addition, the steepness of topography also resulted in decreasing wave heights due to loss of energy as described in the results and discussion section. Finally, the results of impacts of the WSC obtained from this work will provide necessary data to study the coastal erosion caused by waves, and also the sediment transport and morphological evolution in the future.

5. Acknowledgements

The author would like to acknowledge the Earth System Science (ESS) Cluster, The Joint Graduate School of Energy and Environment (JGSEE), King Mongkut's University of Technology Thonburi for kindly providing 2011 research fund to Dr. Worachat Wannawong. The author is thankful to Cdr. Wiriya Lueangaram for providing the numerical oceanic model codes and datasets. Finally, the author is greatly indebted to Mr. Michael Willing and Dr. Donlaporn Saetae for their English proofreading of my book chapter.

6. References

- Allen, J. (2006). *NASA Earth Observatory, using data provided courtesy of the MODIS Rapid Response Team*, Goddard Space Flight Center, Retrieved on December 3, 2006 from <http://earthobservatory.nasa.gov/NaturalHazards/view.php?id=17699&oldid=14009>
- Amante, C. & Eakins, B.W. (2008). *1 Arc-minute global relief model: procedures, data sources and analysis (ETOPO1)*, NOAA, National Geophysical Data Center, Boulder, Colorado, U.S.A.
- Barber, N.F. & Ursell, F. (1948). The generation and propagation of ocean waves and swell, Part-I.; Wave periods and velocities. *Philosophical Transactions of the Royal Society of London-Series A: Mathematical and Physical Sciences* 240: 527-560.

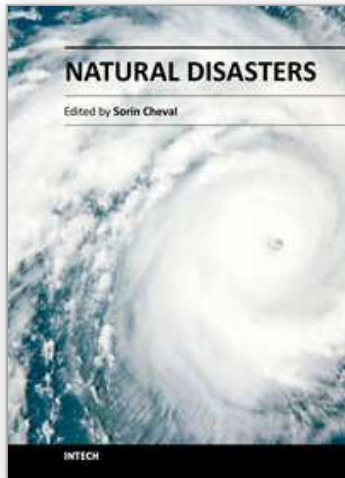
- Blumberg, A.F. & Mellor, G.L. (1987). A description of a three-dimensional coastal ocean circulation model. In three-dimensional coastal ocean models, Heaps, N.S. (Ed.). *Coastal and Estuarine Sciences, American Geophysical Union* 4: 1-16.
- Bowden, K.F. (1983). *Physical oceanography of coastal waters*, Ellis Horwood, Southampton, UK, 302 p.
- Chu, P.C.; Qi, Y.Q.; Chen, Y.C.; Shi, P. & Mao, Q.W. (2004). South China Sea wind-wave characteristics, Part-I.; Validation of WaveWatch-III using TOPEX/Poseidon data. *Journal of Atmospheric and Oceanic Technology* 21: 1718-1733.
- Edwards, M. O. (1989). *Global gridded elevation and bathymetry on 5-minute geographic grid (ETOPO5)*, NOAA, National Geophysical Data Center, Boulder, Colorado, U.S.A.
- Ekphitsuntorn, P.; Wongwiset, P.; Chinnarasri, C.; Humphries, U.W. & Vongvisessomjai, S. (2010). Numerical modeling of erosion for muddy coast at Bangkhuntien shoreline, Thailand. *International Journal of Environmental Science and Engineering* 4: 230-240.
- Harr, P.; Ellsberry, R.; Hogan, T.F. & Clune, W. (1992). North Pacific cyclone sea-level pressure errors with NOGAPS. *Weather and Forecasting* 7: 3-7.
- Hasselmann, K.; Barnett, T.P.; Bouws, E.; Carlson, H.; Cartwright, D.E.; Enke, K.; Ewing, J.I.; Gienapp, H.; Hasselmann, D.E.; Kruseman, P.; Meerbrug, A.; Muller, P.; Olvers, D.J.; Richter, K.; Sell, W. & Walden, H. (1973). Measurements of wind-wave growth and swell decay during the Joint North Sea Wave Project (JONSWAP). *Deutsche Hydrographische Zeitschrift* 8: 95-105.
- Hasselmann, S.; Hasselmann, K.; Bauer, E.; Janssen, P.A.E.M.; Komen, G.J.; Bertotti, L.; Lionello, P.; Guillaume, A.; Cardone, V.C.; Greenwood, J.A.; Reistad, M.; Zambresky, L. & Ewing, J.A. (1988). The WAM model—a third generation ocean wave prediction model. *Journal of Physical Oceanography* 12(18): 1775-1810.
- Hogan, T.F. & Rosmond, T.E. (1991). The description of the navy operational global atmospheric system's spectral forecast model. *Monthly Weather Review* 8(119): 1786-1815.
- Holt, B.; Liu, A.K.; Wang, D.W.; Gnanadesikan, A. & Chen, H.S. (1998). Tracking storm generated waves in the northeast Pacific Ocean with ERS-1 synthetic aperture radar imagery and buoys. *Journal of Geophysical Research: Oceans* 103: 7917-7929.
- Hwang, P.A. & Wang, D.W. (2001). Directional distributions and mean square slopes in the equilibrium and saturation ranges of the wave spectrum. *Journal of Physical Oceanography* 31: 1346-1360.
- Komen, G.; Cavaleri, L.; Donelan, M.; Hasselmann, K.; Hasselmann, S. & Janssen, P.A.E.M. (1994). *Dynamics and modelling of ocean waves*, Cambridge University Press, Cambridge, 532 p.
- Large, W.G. & Pond, S. (1981). Open ocean momentum fluxes in moderate to strong winds. *Journal of Physical Oceanography* 11: 324-336.
- Levitus, S. & Boyer, T. (1994). *World Ocean Atlas: Temperature*, NOAA Atlas NESDIS 4. U.S. Government Printing Office 4: 117-118.
- Levitus, S.; Burgett, R. & Boyer, T. (1994). *World Ocean Atlas: Salinity*, NOAA Atlas NESDIS 3. U.S. Government Printing Office 3: 99-100.

- Moon, I.; Ginis, I.; Hara, T.; Tolman, H.L.; Wright, C.W. & Walsh, E.J. (2003). Numerical simulation of sea surface directional wave spectra under Hurricane wind forcing. *Journal of Physical Oceanography* 33: 1680-1706.
- Powell, M.D.; Vivkery, P.J. & Reinhold, T.A. (2003). Reduced drag coefficient for high wind speeds in tropical cyclones. *Nature* 422: 278-283.
- Pugh, T.D. (1987). *Tides, surges and mean sea-level*, John Wiley & Sons, London, UK, 472 p.
- Tolman, H.L. (1991). A third-generation model for wind-waves on slowly varying, unsteady, and Inhomogeneous depths and currents. *Journal of Physical Oceanography* 21: 782-797.
- Walsh, E.J.; Hancock, D.W.; Hines, D.E.; Swift, R.N. & Scott, J.F. (1989). An observation of the directional wave spectrum evolution from shoreline to fully developed. *Journal of Physical Oceanography* 19: 670-690.
- Wannawong, W.; Humphries, W.U. & Luadsong, A. (2008). The application of curvilinear coordinate for primitive equation in the Gulf of Thailand. *Thai Journal of Mathematics* 6: 89-108.
- Wannawong, W.; Humphries, W.U. & Wongwises, P. (2010a). Optimization of bathymetry database for coastal areas. *Journal of Mathematics and Statistics* 6(3): 286-293.
- Wannawong, W.; Humphries, W.U.; Wongwises, P.; Vongvisessomjai, S. & Lueangaram, W. (2010b). A two-dimensional wave prediction model along the best track of Typhoon Linda 1997. *American Journal of Environmental Sciences* 6(3): 280-285.
- Wannawong, W.; Humphries, W.U.; Wongwises, P.; Vongvisessomjai, S. & Lueangaram, W. (2010c). A numerical study of two coordinates for energy balance equations by wave model. *Thai Journal of Mathematics* 1(8): 197-214.
- Wannawong, W.; Humphries, W.U.; Wongwises, P.; Vongvisessomjai, S. & Lueangaram, W. (2010d). Numerical analysis of wave and hydrodynamic models for energy balance and primitive equations. *International Journal of Mathematical and Statistical Sciences* 4: 140-150.
- Wannawong, W.; Humphries, W.U.; Wongwises, P.; Vongvisessomjai, S. & Lueangaram, W. (2010e). Numerical modeling and computation of storm surge for primitive equation by hydrodynamic model. *Thai Journal of Mathematics* 8: 347-363.
- Wannawong, W.; Humphries, W.U.; Wongwises, P. & Vongvisessomjai, S. (2011a). Mathematical modeling of storm surge in three dimensional primitive equations. *International Journal of Computational and Mathematical Sciences* 1: 44-53.
- Wannawong, W.; Humphries, W.U.; Wongwises, P. & Vongvisessomjai, S. (2011b). Three steps of one-way nested grid for energy balance equation by wave model. *International Journal of Computational and Mathematical Sciences* 1: 23-30.
- Wannawong, W.; Wongwises, P.; Ekphisutsuntorn, P.; Ekkawatpanit, C. & Humphries, W.U. (2011c). Numerical study of the effect of wind-waves generated by tropical cyclones using wave model. Section: Storm surge and waves, Solutions to coastal disasters 2011, Conference proceeding paper. *American Society of Civil Engineers* 1: 149-163.
- Wittmann, P.A. & Farrar, P.D. (1997). Global, regional and coastal wave prediction. *Marine Technology Society Journal* 1(31): 76-82.

Wright, C.W.; Walsh, E.J.; Vandemark, D.; Krabill, W.B.; Garcia, A.W.; Houston, S.H.; Powell, M.D.; Black, P.G. & Marks, F.D. (2001). Hurricane directional wave spectrum spatial variation in the open ocean. *Journal of Physical Oceanography* 31: 2472-2488.

IntechOpen

IntechOpen



Natural Disasters

Edited by Dr. Sorin Cheval

ISBN 978-953-51-0188-8

Hard cover, 156 pages

Publisher InTech

Published online 02, March, 2012

Published in print edition March, 2012

The crossroads between a more and more populated human communities and their changing environment pose different challenges than ever before. Therefore, any attempt to identify and deliver possible solutions is more than welcome. The book *Natural Disasters* addresses the needs of various users, interested in a better understanding of hazards and their more efficient management. It is a scientific enterprise tackling a variety of natural hazards potentially deriving into disasters, i.e. tropical storms, avalanches, coastal floods. The case studies presented cover different geographical areas, and they comprise mechanisms for being transferred to other spots and circumstances. Hopefully, the book will be beneficial to those who invest their efforts in building communities resilient to natural disasters.

How to reference

In order to correctly reference this scholarly work, feel free to copy and paste the following:

Worachat Wannawong and Chaiwat Ekkawatpanit (2012). Tropical Cyclone Wind-Wave, Storm Surge and Current in Meteorological Prediction, *Natural Disasters*, Dr. Sorin Cheval (Ed.), ISBN: 978-953-51-0188-8, InTech, Available from: <http://www.intechopen.com/books/natural-disasters/tropical-cyclone-wind-wave-storm-surge-and-current-in-meteorological-prediction>

INTECH
open science | open minds

InTech Europe

University Campus STeP Ri
Slavka Krautzeka 83/A
51000 Rijeka, Croatia
Phone: +385 (51) 770 447
Fax: +385 (51) 686 166
www.intechopen.com

InTech China

Unit 405, Office Block, Hotel Equatorial Shanghai
No.65, Yan An Road (West), Shanghai, 200040, China
中国上海市延安西路65号上海国际贵都大饭店办公楼405单元
Phone: +86-21-62489820
Fax: +86-21-62489821

© 2012 The Author(s). Licensee IntechOpen. This is an open access article distributed under the terms of the [Creative Commons Attribution 3.0 License](#), which permits unrestricted use, distribution, and reproduction in any medium, provided the original work is properly cited.

IntechOpen

IntechOpen